Pergamon

Int. J. Solids Structures Vol. 35, No. 19, pp. 2413–2427, 1998

0020–7683/98 $19.00 + .00

PII: S0020–7683(97)00140–6

TOPOLOGICAL DISORDER OF MICROSTRUCTURE AND ITS RELATION TO THE STRESS FIELD

R. PYRZ
Institute of Mechanical Engineering, Aalborg University, Pontoppidanstræde 101, 9220 Aalborg, Denmark
E-mail: rp@ime.auc.dk

and

B. BOCHENEK
Institute of Mechanics and Machine Design, Cracow University of Technology, Warszawska 24, 31-155 Cracow, Poland

(*Received* 19 *May* 1997)

Abstract—This paper addresses the problem encountered in the quantitative description of arrangements and correlations in unidirectionally reinforced composite materials. Both topological and second-order statistical measures are related to the stress variability that exists under transverse loading conditions. The main attention is paid to the variability of interfacial maximal radial stresses which are primary sources of an interfacial debonding. Correlation measures have been suggested for global, as well as local, correlations. It is shown that a further improvement of the local correlation measures is necessary if it is going to be used as a diagnostic tool to pinpoint most loaded, local areas of the microstructure. © 1998 Elsevier Science Ltd. All rights reserved.

1. INTRODUCTION

Variability of the arrangement of microstructural features and their mutual interaction determines physical characteristics of materials. This is particularly true for the description of strongly non-linear phenomena such as fracture, where the short range interactions between microstructural entities play a dominant role in non-homogeneous local variations of field quantities. For not dilute concentrations the interaction effects between neighbouring inclusions are highly influential on the overall behaviour of the material. Consequently, it is important to develop a framework which would allow to classify different types of inclusion dispersions and provide a quantitative information related to spatial distribution of inclusions.

If the material is statistically homogeneous, which means that the local material properties are constant when averaged over a representative volume element, then it is possible to replace the real disordered material by a homogeneous one, where the local material properties are the averages over the representative volume element in the original material. Estimation of those averages presents a fundamental issue for different effective medium theories (Nemat-Nasser and Hori, 1993; Chen *et al.*, 1992; Takao *et al.*, 1982; Benveniste, 1987). Usually, the size and the shape of the inclusions are accounted for, but as far as the spatial distribution of inclusions is concerned the salient assumption is made that the inclusions are uniformly distributed in a random fashion. On the other hand, a finite element calculation procedure implies in most cases periodicity of the inclusion's distribution. However, very few microstructures are purely random or perfectly regular. In order to perceive the microstructure of composite materials as it really exists rather than as described by some assumed model, it is necessary to recognize that we have to deal with non-regular, non-random microstructures.

The arrangement of fibres in unidirectional composites can be studied by representing each fibre observable on the transverse sections by an associated centre point, and analyzing the set of points irregularly distributed in the area of observation. Point patterns may be classified using different measures such as neighbour distances and orientations, areas of

conjugate Dirichlet polygons, micromorphological parameters and degree of contiguity (Everett and Chu, 1993; Taya *et al.*, 1991; Altan *et al.*, 1990; Wimolkiatisat *et al.*, 1990; Pyrz, 1993, 1994a). More informative characteristics of the point set are obtained using statistical second-order quantities which examine the association of points relative to other points of the set in an immediate local neighbourhood of the reference point (Ripley, 1977; Pyrz, 1994a; Hanisch *et al.*, 1985; König *et al.*, 1991; Karlsson and Liljeborg, 1994). These quantities are statistically averaged over all the points of the set and, therefore, do not provide a detailed knowledge concerning the local configuration of points. Nevertheless, it is possible to derive several useful parameters such as most frequently occurring distances between points and an averaged number of points lying within a predetermined distance, which may be used for constitutive modelling purposes. Careful analysis of second-order quantities may disclose subtle differences between apparently similar distributions as shown in Pyrz (1995). Topological properties of the pattern are intimately related to morphological analysis of the microstructure in a similar way as the geometrical properties. In the context of point sets, which exemplify distribution of fibres, the point pattern may be replaced in a unique way by conjugate polygonal tessellations. Then the topological properties rather than metric properties of underlying dispersion can be studied and can be related to some physical mechanisms which constitute the microstructure (Rivier, 1985; Weaire and Rivier, 1984; Lemaitre *et al.*, 1993).

Since an ultimate task of material characterization is to find a direct link between microstructures' constitution and physical properties it is desirable to investigate the relations which correlate geometrical and topological properties of the microstructure with field quantities, which exist within the microstructure under imposition of an external loading. Most existing investigations correlate regular or periodic microstructures with overall properties and field quantities [see Böhm and Rammerstorfer (1995); Moulinec *et al.* (1995); Brockenborough *et al.* (1991); Zhu and Achenbach (1991)], and only a few contributions have paid attention to the correlation of physical properties with disordered microstructures [e.g. Siegmund *et al.* (1995); Pyrz (1994b); Stoyan and Schnabel (1990); Pyrz (1997); Torquato (1991); Beran (1968)].

The intent of this work is to describe a convenient framework that allows to estimate geometrical and topological properties of different dispersions of fibres in unidirectional composites and to relate these properties to the stress field under transverse loading conditions.

2. STRESS FIELD

The amount of constituent elements forming the material is in many cases known beforehand as for example the volume fraction of reinforcing phase in composite materials. However, the volume concentration of inclusions is merely a statement of the overall composition of the material rather than of its dispersion characteristics. The final architecture of a microstructure is controlled only to a limited extent, and on the microscale the geometrical arrangement of second-phase inclusions is a result of complex and interacting processing micromechanisms. If the processing conditions are stable and the variability of constituent properties are minimal then we may consider resulted microstructure as statistically homogeneous when sampled at different positions in a body of the material. In simulation experiments three model dispersions have been generated (Fig. 1). A hard-core dispersion arises by the imposition of a minimum permissible distance between any two points which are distributed randomly otherwise. The hard-core one model is obtained by the imposition of the prohibitive distance between points to be significantly larger than the fibres diameter, whereas in the hard-core two model a minimal interpoint distance is equal to the diameter of fibres. This restriction guarantees a large degree of randomness to be present in the hard-core two pattern. The cluster model may be created in many different ways by distributing cluster centres randomly and placing offspring points randomly around parent points within a predetermined area. In this case, cluster area, number of parent points and number of daughter points within each cluster can be randomized. In the present case the cluster distribution possesses 30 parent points and 10 randomly distributed around

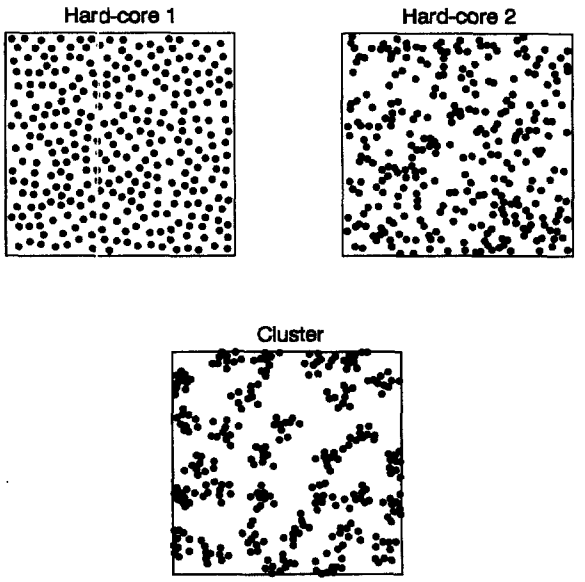

Fig. 1. Dispersion patterns of fibres.

offspring points. The hard-core one and hard-core two distribution models exemplify, respectively, well processed composite and a composite processed with insufficient consolidation pressure that results in decreased penetrability of fibres through the matrix material. The cluster model represents composite reinforced with randomly dispersed bundles of fibres.

The local stress analysis of patterns is reduced to a two-dimensional plain strain problem as the fibres are assumed to be elastic parallely aligned, and embedded in an elastic matrix with perfect bonding (Pijaudier-Cabot and Bažant, 1991).

The stress field solution for a single inclusion embedded in a matrix may be obtained analytically from the Eshelby solution (Mura, 1987). As for the Eshelby solution the eigenstrain analogy is also applied, but contrary to this solution where the Eshelby tensor is solved, an iterative procedure is derived. The heterogeneous solid is replaced by an equivalent homogeneous one where tractions are applied on the imaginary contour of the circular fibre and an unbalanced stress field is added inside the imaginary contour. The stress field inside the fibre is determined by an iterative procedure, and subsequently the stress field in the matrix can be calculated.

In the solution of multiple fibres the stress field interaction between the fibres must be taken into account. The basic idea of accounting for this interaction is to determine the stress field inside a fibre as it would be alone including, however, the interacting stress field from the neighbouring fibres. Then, the problem is divided into a number of subproblems corresponding to the number of fibres (Fig. 2).

Each subproblem is solved as for a single fibre and in addition the interacting stresses from the remaining fibres are included in the stress field calculation inside the area covered by the fibre. The plane solid containing multiple randomly dispersed fibres is subjected to unidirecitonal loading $\boldsymbol{\sigma}_\infty$ at the remote boundaries. The solid contains N fibres all of circular shape, and the boundary curves for the fibres are denoted by Γ_j where $j = 1, \ldots, N$. All the fibres have the same elastic stiffness $\mathbf{D}_a$ and the matrix has the elastic stiffness $\mathbf{D}_m$. Radii of the fibres are all equal to $R = 5\ \mu$m.

As a starting point in the iterative procedure the stress field in the whole solid is equal to remote loading at boundaries $\boldsymbol{\sigma} = \boldsymbol{\sigma}_\infty$. Using the theory of eigenstresses (Mura, 1987), the unbalanced stress field for each fibre becomes:

$$\Delta\boldsymbol{\sigma}_j = (\mathbf{D}_m - \mathbf{D}_a)\mathbf{D}_a^{-1}\boldsymbol{\sigma}_j \quad j = 1, \ldots, N. \tag{1}$$

Tractions are applied at the imaginary contours of the fibres

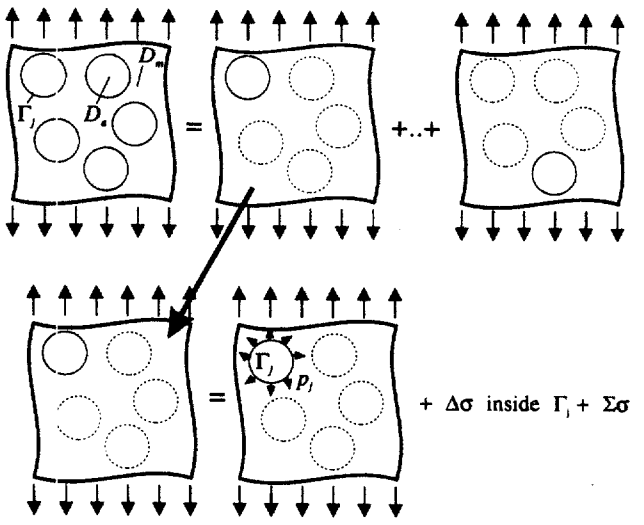

Fig. 2. Superposition scheme for a solid containing multiple fibres.

$$\mathbf{p}_j = -\Delta\boldsymbol{\sigma}_j\mathbf{n}_j \quad j = 1,\ldots,N, \tag{2}$$

when $\mathbf{n}_j$ is an outward unit normal to the circular contour $\boldsymbol{\Gamma}_j$. The boundary curve $\boldsymbol{\Gamma}_j$ is subdivided into segments of length ds, and the tractions $\mathbf{p}_j$ are replaced by concentrated forces $\mathbf{p}_j ds$. By applying the solution for a concentrated force in a homogeneous elastic solid the disturbance stress from $\mathbf{p}_j ds$ is denoted as $\mathbf{f}[\mathbf{p}_j]ds$ along the circular contours

$$\boldsymbol{\sigma}_{ij} = \oint_{\Gamma_i} \mathbf{f}[\mathbf{p}_j]ds \quad j = 1,\ldots,N, \tag{3}$$

and the disturbance stress is calculated at an arbitrary point within the contour. The new stress field inside the fibres is obtained by

$$\boldsymbol{\sigma}_j = \boldsymbol{\sigma}_\infty + \sum_{i=1}^{N} \boldsymbol{\sigma}_{ij} - \Delta\boldsymbol{\sigma}_j \quad \text{inside } \boldsymbol{\Gamma}_j. \tag{4}$$

From this expression the unbalanced stress is re-calculated according to eqn (1), and the iterations are repeated until $\mathbf{p}_j$ does not change significantly. The method converges quite rapidly and the stress field outside the fibre may be determined as follows:

$$\boldsymbol{\sigma}_j = \boldsymbol{\sigma}_\infty + \sum_{i=1}^{N} \boldsymbol{\sigma}_{ij} \quad \text{outside } \boldsymbol{\Gamma}_j. \tag{5}$$

The stress analysis is implemented in a numerical procedure and the stress field at any arbitrary point is obtained within reasonable computational time. It should be noted that every simulated pattern must be equipped with appropriate boundary conditions. Since the dispersion of fibres is observed within a finite window the edge effects may influence the stress field calculations as well as a calculation of geometrical and topological parameters of the dispersion. In order to avoid this problem periodic boundary conditions are applied to all calculations. It means that the window of observation has to be surrounded by a sequence of windows containing the same dispersion patterns as the original one. In other words, we enlarge the space of observation by assuming that the dispersion of fibres in a very large area may be reconstructed from a single window of observation by a sequential repetition of the observation window itself. This keeps the dispersion characteristics fixed and diminishes the edge effects.

Since the initiation of microcracking usually occurs at the fibre–matrix interphase, maximal radial and tangential stresses in an annular layer around each fibre are of particular interest. Figures 3 and 4 illustrate variability of maximal radial and tangential stresses for all fibres of each dispersion types. The stresses have been calculated for both uniaxial as well as biaxial loading. The influence of the dispersion type on the maximal value of radial and tangential stresses is apparent. First of all, fluctuations of stresses are smallest for the hard-core one distribution whereas the cluster distribution contains a number of fibres with significantly larger stress values than other fibres in the pattern. Secondly, maximal radial stresses for all fibres in considered dispersions are amplified with respect to remote unit load, whereas only a certain number of fibres in the hard-core two pattern and a larger number in the cluster pattern are exposed to amplified tangential stresses. It is interesting to notice that the mean value of maximal radial and tangential stresses increases as the dispersion gets more disordered. The local variability of stress maxima is completely hidden in this quantity. Imposition of the biaxial loading to the patterns does not alter significantly maximal radial stresses, and if anything, the slight decrease of stress intensity is observed, however, the picture of maximal tangential stresses changes dramatically. The values of maximal tangential stresses are magnified almost twice as compared to the uniaxial loading. Thus, it is most likely that maximal radial stress hot spots alone generated under uniaxial

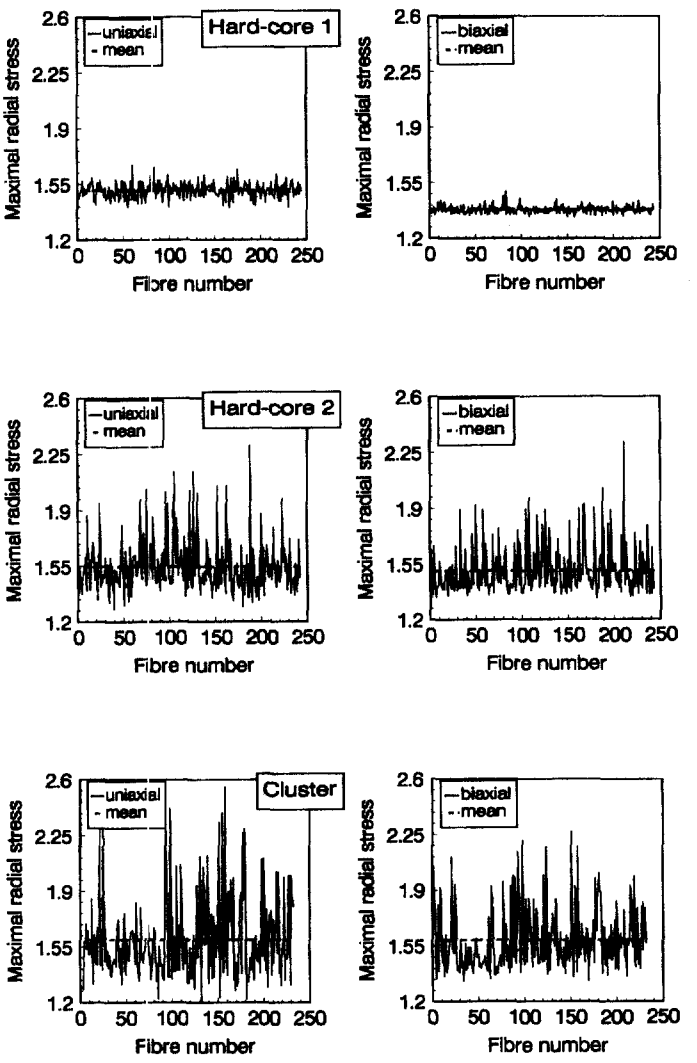

Fig. 3. Variability of maximal radial stresses among fibres in uniaxial and biaxial loading.

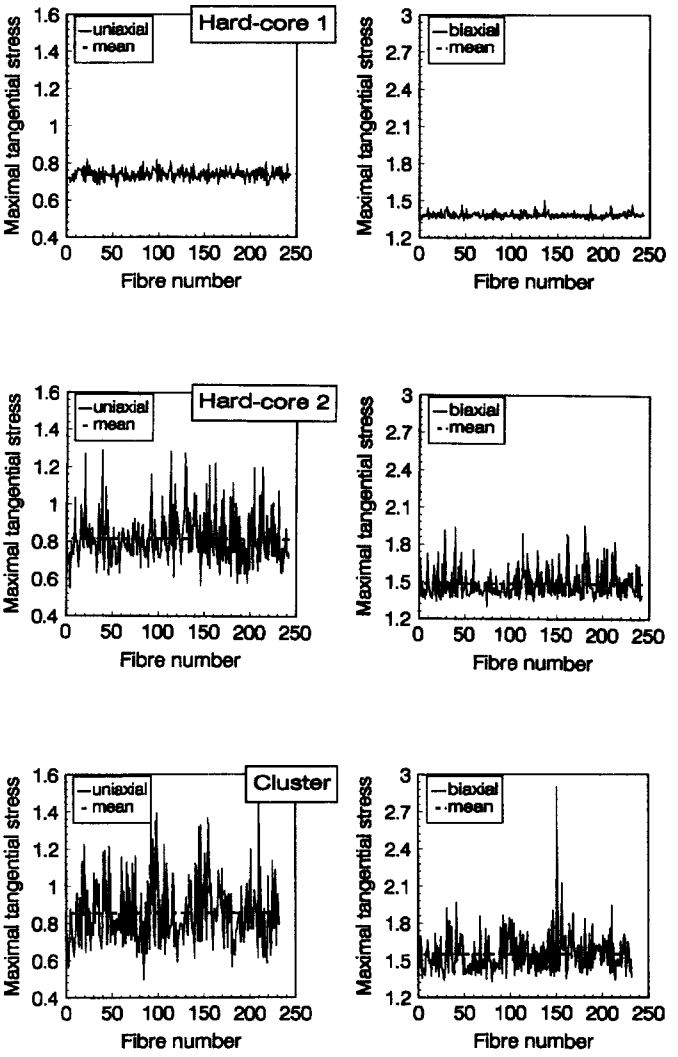

Fig. 4. Variability of maximal tangential stresses among fibres in uniaxial and biaxial loading.

loading are strong enough to initiate interfacial debonding, provided that the matrix strength is higher than the strength of the interphase. Furthermore, it is expected that increased intensity of both radial and tangential maximal stresses under biaxial loading would initiate radial matrix cracks combined with interfacial debonding. In the following analysis the attention will be paid exclusively to maximal radial stresses under uniaxial loading conditions.

Amplification of local maximal radial stresses and their variability is related to nearest neighbour distances and nearest neighbour orientations of adjacent fibres. An average nearest neighbour distance between fibres in the hard-core one model is larger than for two other models and this tendency is prevailed for all nearest neighbour orientations where the loading direction corresponds to 90° (Fig. 5). The inter-fibre distances in the cluster model are significantly smaller and vary with orientation to a larger extent than in the hard-core distributions. Since the interaction effects are strongly influenced by the distances between neighbouring fibres, as will be shown in a sequel, the stress amplification is much more pronounced in the cluster model than in the other two models. Furthermore, the amplification of the maximal radial stresses is largest for fibres which are aligned very close or along the loading direction. There are more fibres in the cluster model which are mutually positioned along the loading direction at shorter distances than in other models. This has

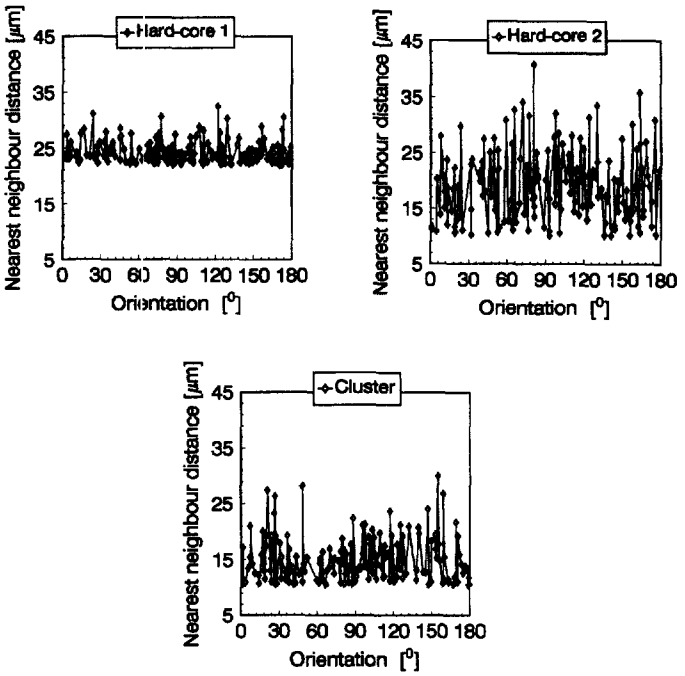

Fig. 5. Variability of nearest neighbour distances vs orientation for different distributions.

resulted in larger variability of maximal radial stresses among the fibres dispersed in the form of clusters.

3. GLOBAL CORRELATIONS

Statistical fluctuations of interfacial stresses are caused by a geometrical disorder of the microstructure. A system is weakly disordered if the disorder disappears when one samples the system at progressively smaller or larger scales. In strongly disordered systems the disorder persists at all scale lengths. Furthermore, some of the physical processes may be dependent upon the system size, as well. In the present investigation the system is fixed with respect to the size of the observation window and the number of microstructural entities under consideration, i.e. number of inclusions. Thus, the fibre volume fraction is the same for all simulations in order to eliminate an eventual effect of fibres density. It is expected that varying fibre volume fraction may change a quantitative picture of relations between stresses and/or topological and geometrical properties of considered distributions preserving, however, qualitative characteristics of correlations. Then we consider the window of observation as a statistically representative area. It is in this area where we seek to find correlations between global descriptors of disorder and the stress variability.

Figure 6 illustrates transformation of the point set onto the set of contiguous polygons. This construction, referred to as the Dirichlet tessellation, defines uniquely neighbours of the fibres. Each fibre is assigned a polygonal cell enclosing all points which are closer to the reference fibre than to any other fibre. The sides of the enclosing polygon are obtained from the set of perpendicular bisectors of the line segments that connect the enclosed fibre with neighbouring fibres. Boundary polygons which have a fragment of the window frame as one of the edges are excluded from the analysis. This is because their topology and geometry is not solely defined by a point set but is artificially constrained due to a finite size of the observation window.

Several metric properties of polygonal sets may now be investigated for different dispersions such as distribution of cell areas, perimeters, elongation, etc. In geometrical terms, all random cellular structures generated by the same point set model are indistinguishable, even if they are not identical when superimposed. Therefore, the polygons

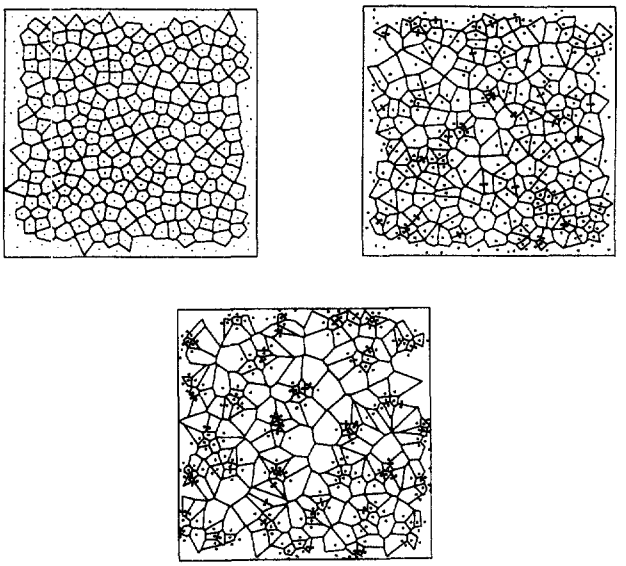

Fig. 6. Dirichlet tessellations for three distributions.

cannot be defined and distinguished by their size or any other metric measure alone. Their distinctive feature is their shape which is a topological property. Aiming to describe the topological randomness of the pattern, the topological shape of a polygon, i.e. the number of its sides, is considered as the random variable. Then the polygonal tessellation is described by the frequencies p_n of finding an n-sided polygon (Fig. 7). Statistical status of the polygonal network may be characterized by the topological entropy (Rivier, 1985)

$$S = -\sum_{n=1}^{k} p_n \ln p_n \tag{6}$$

The topological entropy measures a degree of arbitrariness. The entropy value for a perfectly regular pattern is always equal to zero and grows with an increasing disorder. It is also a remarkable property of polygonal tessellations that the average number of polygon sides is six and this value is conserved regardless of the degree of disorder of the underlying point pattern. Thus the frustration of the random network of polygons, i.e. growing topological entropy is caused by an appearance of polygons with a number of edges different

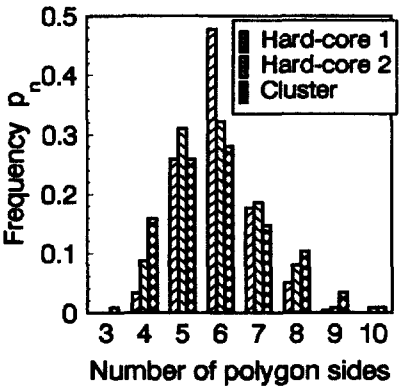

Fig. 7. Frequency distribution of n-sided polygons for considered patterns.

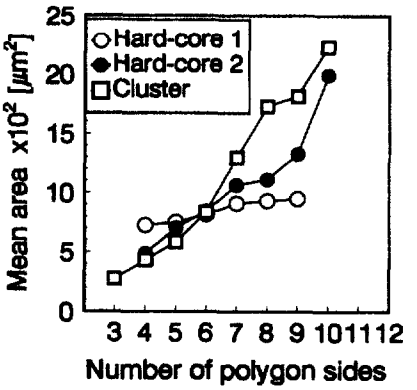

Fig. 8. Mean area of n-sided polygons vs number of polygon sides.

from six. Figure 8 shows the relation between the size of polygons and their topological shape. Independent of the degree of disorder the mean area of n-sided polygons grows with the number of polygon sides. This property may be derived from eqn (6) supplied with normalization, space filling and topological constraints (Rivier, 1985). It is to be noticed that the mean area of six-sided polygons is almost identical for considered patterns. Thus, one could consider polygons with the number of sides different from six as topological defects which influence the value of topological entropy as well as enlarge the variability of the stress field depending on the degree of disorder. For example, the existence of many small four-sided and large eight-sided polygons in the cluster model (Figs 7 and 8), increases significantly the value of topological entropy as compared with the hard-core models. Simultaneously, the reference fibre enclosed by the four-sided polygon has a big chance of being close to other fibres since its "territory", i.e. the area of the polygon, is on average smaller than other polygons. On the other hand, the fibre contained within the eight-sided polygon has much more freedom as far as its location is concerned. However, there are many more eight-sided polygons in the cluster model than in the hard-core models and, therefore, the probability of those fibres to be closer located to their neighbours in the cluster model is larger than in the hard-core models. These considerations suggest that the topological defects may have an effect on the amplification of interfacial stresses and their variability. The global correlation between stress field and topology expressed in terms of the coefficient of variation and the topological entropy is shown in Fig. 9. The coefficient of variation is defined as the ratio of standard deviation to mean value of maximal radial stresses. This figure illustrates the results of different simulations where several realizations of three models have been performed according to procedures described previously. The

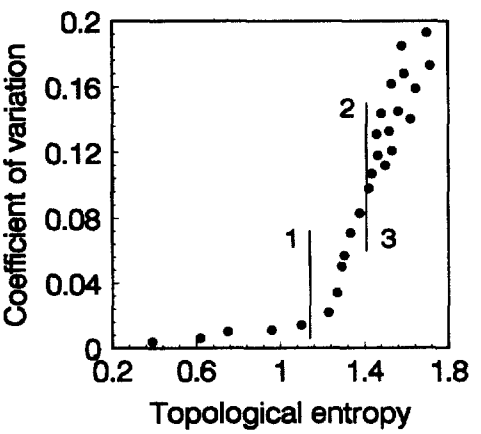

Fig. 9. Correlation between topological entropy and maximal radial stresses.

graph is divided into three areas corresponding to hard-core 1 (1), hard-core 2 (2) and cluster (3) models, respectively. Variability of the stress field increases with increasing topological disorder in agreement with results shown in Fig. 3. The large dispersion of the results for the cluster model is probably caused by a variety of different cluster realizations as far as a number of parent and offspring points as well as areas of clusters are concerned.

An appealing alternative to describe global correlations in point fields is a multivariate characterization of patterns by second-order quantities (Stoyan and Stoyan, 1994). In addition to positions of fibres we introduce a further variable to be the "mark" of the fibre with a given position. The mark represents a typical feature expressible by numbers which may correspond to the size, shape of fibres or any field quantity known at the fibre spot. In the present context the maximal radial stresses at fibres' interphases are taken as marks. The mark correlation function $M(r)$ corresponds to the conditional mean value of the marks' product of a pair of fibres positioned r distance apart. Construction of the mark correlation function is shown in Fig. 10. First, one calculates the second-order mark intensity function $H(r)$ which describes the mean value of the pair products of marks m_k attached to the points within a circular area r

$$H(r) = \frac{1}{m^2}\frac{A}{N^2}\sum_{i=1}^{N} h_i \tag{7}$$

where m is the mean value of marks in the observation area A, and h_i is a sum of mark products between the ith point at the centre of the circular area r and all points lying within it, i.e.

$$h_i = \sum_{k=1}^{k^i} m_i m_k. \tag{8}$$

Components h_i are calculated for all N points as centres and the procedure is repeated for increasing values of radius r. Taking the derivative of the mark intensity function $H(r)$ with respect to r, one obtains the mark correlation function $M(r)$ (Fig. 11). Sharp peaks present in the graphs suggest a strong correlation (amplification) of marks' value at corresponding distances. These distances are related to average nearest neighbour distances (see Fig. 5). The larger peak values, the stronger attraction exists between marks in the pattern as exemplified by the cluster model. The mark correlation function fluctuates tending to unity at larger distances indicating that no further correlation exists at those distances. The limiting distance, where $M(r)$ starts to fluctuate around unity without any distinct appearance of peaks and valleys, determines the correlation length of a given pattern. The clear minimum of $M(r)$ at distances equal to 60 μm indicates a gap in the correlation at those distances which represent a separation distance between clusters. The information contained in the mark correlation function is averaged over the observation window and hence

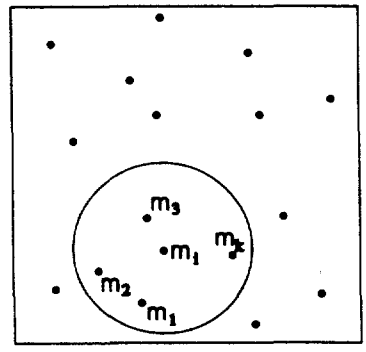

Fig. 10. Construction of the mark correlation function.

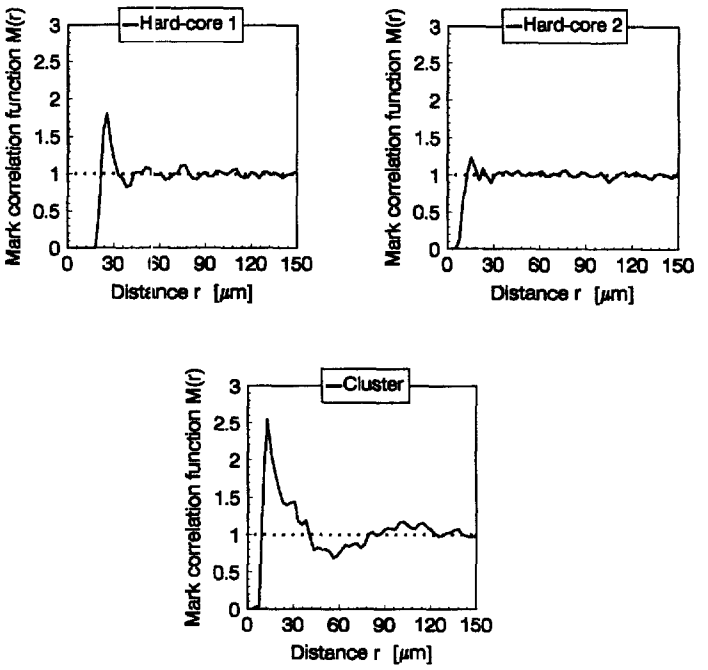

Fig. 11. Mark correlation functions for considered patterns.

provides only global correlations that might exist in the pattern in a similar manner as topological correlations do.

4. LOCAL CORRELATIONS

Statistically averaged topological and second-order functions presented in the previous chapter precluded to draw any conclusion that refers to local values of field quantities. Established correlations are valid at scale lengths which are equal or larger than the window of observation. Local correlations can only be determined if we find relations between a short-range configuration of fibres described by a suitably chosen measure and corresponding values of field quantities.

Pairwise interactions between neighbouring fibres and pairwise location correlations are fundamental building blocks in the global correlation scheme. For a single pair of fibres located a distance d apart and having radius $R = 1$ amplification of maximal radial stresses at the reference fibre is largest for small inter-fiber distances and, in the case of uniaxial loading, when the fibres are aligned along loading direction (Fig. 12). An angular deviation of the neighbouring fibre from the loading direction decreases the degree of interaction between fibres and results in lower maximal radial stresses of the reference fibre. If the

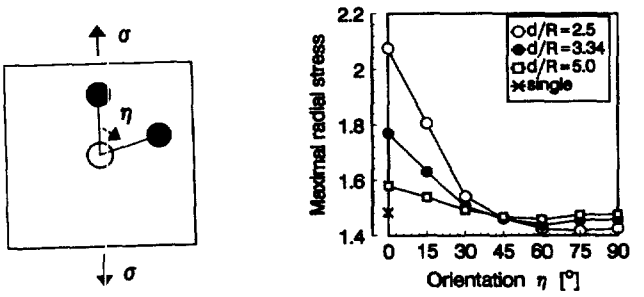

Fig. 12. Maximal radial stresses for the pair of fibres.

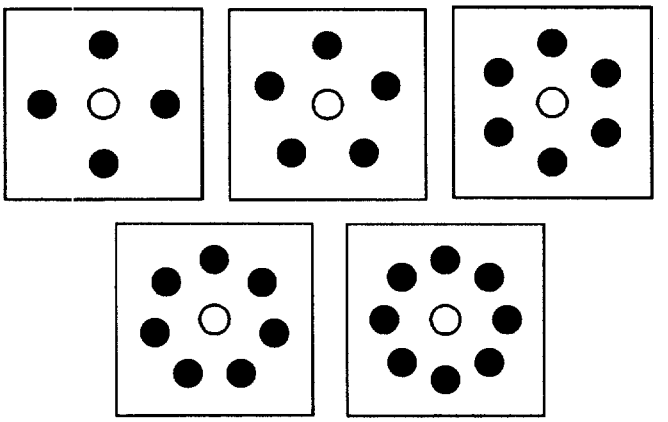

Fig. 13. Distribution of neighbouring fibres for n-sided regular polygons.

reference fibre is surrounded by regularly placed $4, 5 \ldots 8$ neighbours (Fig. 13), i.e. the neighbours are at vertices of the regular quadrilateral, pentagon ... octagon, then the maximal radial stress intensifies as the number of polygon edges decreases (Fig. 14). Thus the surrounding neighbours have a screening effect on the reference fibre. However, it has to be remembered that this effect is present in regular configuration of neighbours, whereas such configuration is very unlikely to occur in simulated distribution models. Furthermore, the reference fibre is not necessarily located at the centre of the polygon and it may happen that the eccentricity is so large that the interaction effect from the nearest fibre totally overshadows influence of the remaining fibres composing the polygonal cell. Nevertheless, these effects can be captured again by the pairwise interaction between the reference fibre and its neighbours.

Introducing a correlation parameter as

$$C = \min_i(\min_j C_{ij}) \tag{9}$$

where

$$C_{ij} = d_{ij}\left(1 + \frac{\theta_{ij}}{\alpha}\right) \tag{10}$$

one tries to find a correspondence between stress interaction effects and geometrical parameters d_{ij} and θ_{ij} which represent a length of centre line and its orientation with respect to

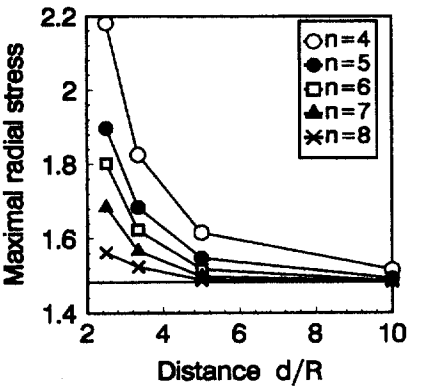

Fig. 14. Maximal radial stress of the reference fibre with n neighbours.

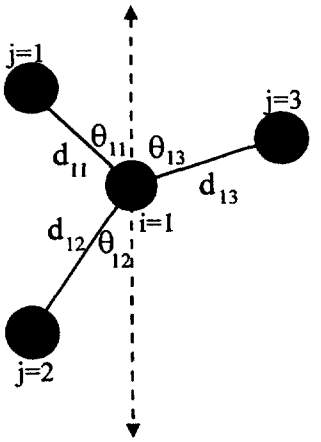

Fig. 15. Local distribution parameters.

the loading direction (Fig. 15). Normalizing factor α is equal 60° which is the centre line's declination angle at which the pair of fibres ceases to interact (see Fig. 12). The minimal correlation parameter is found among neighbours j of the reference fibre i for all $i = 1, \ldots, N$. The smallest value C should correspond to the largest value of maximal radial stresses among all fibres in the pattern, provided eqn (10) is valid and only pairwise interactions are taken into account. Figure 16 gives two examples of the correlation parameter's validity. Fibres exposed to largest maximal radial stresses may come in pairs if they are mutually nearest neighbours or as singles otherwise. The correlation parameter is sensitive enough if stress differences among fibres are larger than say 10%. Then corresponding differences of C values are large, as well, and an identification of the stress hot spots is unique. However, the situation gets worse if stress differences are small. For example one would wish to pin point 10 fibres with highest maximal radial stresses among all fibres of the hard-core model. The stress range for these ten fibres is from 1.659 for fibre number 1–1.527 for fibre number 10. Corresponding values of C are 11.45 and 13.25, respectively, thus still according to expectations. However, the smallest value of the correlation coefficient is related to the fibre exposed to the maximal radial stress equal to 1.627 which is third largest. Moreover, there are twelve other fibres with correlation coefficient smaller than 13.25 (as for the 10th fibre) despite the fact that fibres' stresses are slightly larger than the stress of the 10th fibre. In other words, the coefficient of correlation selects more fibers than it would be suggested from the stress analysis. This frustration is caused by insufficient differences of stresses in the 10 most loaded fibres. It is simultaneously observed that the differences of distance d_{ij} for selected fibres are very small, as well. In such a situation secondary correlations may be decisive which means that the correlation coefficient C_{ij} should depend further on the configuration of fibres which surround each j fibre.

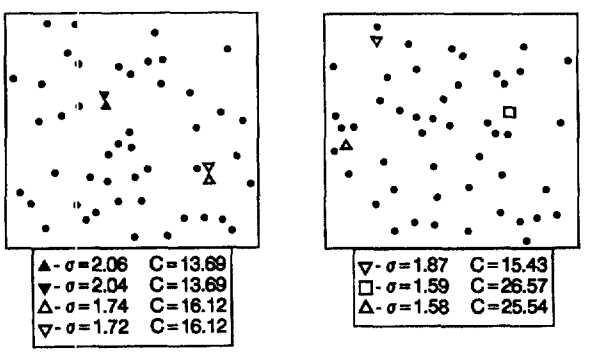

Fig. 16. Detection of local stress hot spots.

5. CONCLUDING REMARKS

The framework that quantifies the distribution of inclusions and allows for the determination of most important aspects of microstructure's disorder is prerequisite for a rigorous statistical assessment of the microstructure arrangement and its relation to the field quantities. Methodology presented here may be extended further in several respects. For example, the global correlations between stresses and topology rely upon the coefficient of variation that is supposed to represent a variability of the stress field. This statement is, however, overestimated in the sense that the coefficient of variation includes only first two moments of the stress distribution whereas a more precise description of the stress distribution would necessitate an involvement of higher-order moments of the distribution or their combinations. In any case, the global stress estimator should always have a clear physical interpretation which could be difficult to achieve with higher moments of the stress distribution, except perhaps first four statistical moments. The concept of local geometrical descriptor C seems to be worth a further development. Its simple linear form should be replaced by a more elaborate, nonlinear expression determined from many realizations of polygonal unit cells surrounded by next near neighbour fibres. Then the second order correlations would be automatically taken care of. A successful selection of reliable local correlation coefficients would provide a diagnostic measure of local load bearing capacity of microstructures.

Problems posed in the present paper and related to classification of inclusion distribution, determination of topological and geometrical quantities which decisively influence the overall and local properties of materials and the exploration of a scaling law which allows to cross boundaries between different length scales, all belong to the area of research that awaits a further development.

REFERENCES

Altan, B., Misirli, Z. and Yorucu, H. (1990) The determination of the homogeneity in multiphase mixtures. *Zeitschrift für Metallkunde* **81,** 221–228.

Axelsen, M. S. and Pyrz, R. (1995) Effect of microcrack formation in transversely loaded unidirectional composites. *Proceedings of the ASME Materials Division* **61-1,** 239–248.

Benveniste, Y. (1987) A new approach to the application of Mori–Tanaka theory in composite materials. *Mechanical Materials* **6,** 147–157.

Beran, M. J. (1968) *Statistical Continuum Theories*. Wiley, New York.

Böhm, H. J. and Rammerstorfer, F. G. (1995) Fiber arrangement effects on the microscale stresses of continuously reinforced MMCS. *Proceedings of the IUTAM Symposium on Microstructure–Property Interactions in Composite Materials*, ed. R. Pyrz. Kluwer, Dordrecht, pp. 51–62.

Brockenborough, J. R., Suresh, S. and Wienecke, H. A. (1991) Deformation of metal matrix composites with continuous fibers: geometrical effects of fiber distribution and shape. *Acta Metallica Materiala* **39,** 735–752.

Chen, T., Dvorak, G. J. and Benveniste, Y. (1992) Mori–Tanaka estimates of the overall elastic moduli of certain composite materials. *Journal of Applied Mechanics* **59,** 539–546.

Everett, R. K. and Chu, J. M. (1993) Modeling of non-uniform composite microstructure. *Journal of Composite Materials* **27,** 1128–1144.

Hanish, K.-H., König, D. and Stoyan, D. (1985) The pair correlation function of point and fibre systems and its stereological determination of planar sections. *Journal of Microscopy* **140,** 361–370.

Karlsson, L. M. and Liljeborg, A. (1994) Second-order stereology for pores in translucent alumina studies by confocal scanning laser microscopy. *Journal of Microscopy* **175,** 186–194.

König, D., Carvajal-Gonzalez, S., Downs, A. M., Vassy, J. and Rigaut, J. P. (1991) Modelling and analysis of 3-D arrangements of particles by point process with examples of application to biological data obtained by confocal scanning light microscopy. *Journal of Microscopy* **161,** 405–433.

Lemaitre, J., Gervois, A., Troadec, J. P., Rivier, R., Ammi, M., Oger, L. and Bideau, D. (1993) Arrangement of cells in Voronoi tesselations of monosize packing of discs. *Philosophical Magazine B* **67,** 347–362.

Moulinec, M. and Suquet, P. (1995) A FFT-based numerical method for computing the mechanical properties of composites from images of their microstructures. *Proceedings of the IUTAM Symposium on Microstructure–Property Interactions in Composite Materials*, ed. R. Pyrz. Kluwer, Dordrecht, pp. 235–246.

Mura, T. (1987) *Micromechanics of Defects in Solids*, Kluwer Academic, Dordrecht.

Nemat-Nasser, S. and Hori, M. (1993) *Micromechanics: Overall Properties of Heterogeneous Materials*. North-Holland, Amsterdam.

Pijaudier-Cabot, G. and Bažant, Z. P. (1991) Crack interacting with particles of fibres in composite materials. *ASCE Journal of Engineering Mechanics* **117,** 1611–1630.

Pyrz, R. (1993) Stereological quantification of the microstructure morphology for composite materials. *Proceedings of the IUTAM Symposium on Optimal Design with Advanced Materials*, ed. P. Pedersen. Elsevier, Oxford, pp. 81–95.

Pyrz, R. (1994a) Quantitative description of the microstructure of composites. Part I: morphology of unidirectional composite systems. *Composite Science Technology* **50,** 197–208.

Pyrz, R. (1994b) Correlation of microstructure variability and local stress field in two-phase materials. *Material Science Engineering* **A177,** 253–259.

Pyrz, R. (1995) Morphology and fracture of disordered composite microstructures. *Proceedings of ICCM 10*, Whistler, Canada, pp. I463–I469.

Pyrz, R. (1997) Fractal characterization of second-phase dispersion in composite materials. *Journal of Science and Engineering of Composite Materials* **6**(3).

Ripley, B. D. (1977) Modelling spatial patterns. *Journal of the Royal Statistical Society, Ser. B* **39,** 172–212.

Rivier, N. (1985) Statistical crystallography; structure of random cellular networks. *Philosophical Magazine B* **52,** 795–819.

Siegmund, T., Fisher, F. D. and Werner, E. A. (1995) Microstructure characterization and FE-modelling of plastic flow in a duplex steel. *Proceedings of the IUTAM Symposium on Microstructure–Property Interactions in Composite Materials*, ed. R. Pyrz. Kluwer, Dordrecht, pp. 349–360.

Stoyan, D. and Schnabel, H.-D. (1990) Description of relations between spatial variability of microstructure and mechanical strength of alumina ceramics. *Ceramics International* **16,** 11–18.

Stoyan, D. and Stoyan, M. (1994) *Fractals, Random Shapes and Point Fields*. Wiley, New York.

Takao, Y., Chou, T. W. and Taya, M. (1982) Effective longitudinal Young's modulus of misoriented short fiber composites. *Journal of Applied Mechanics* **49,** 536–540.

Taya, M., Muramatsu, K., Lloyd, D. J. and Watanabe, R. (1991) Determination of distribution patterns of fillers in composites by micromorphological parameters. *JSNE International Journal* **34**(2).

Torquato, S. (1991) Random heterogeneous media: microstructure and improved bounds on effective properties. *Applied Mechanics Review* **44,** 37–76.

Weaire, D. and Rivier, N. (1984) Soap, cells and statistics-random patterns in two dimensions. *Contemporary Physics* **25,** 59–99.

Wimolkiatisak, A. S., Bell, J. P., Scola, D. A. and Chang, J. (1990) Assessment of fiber arrangement and contiguity in composite materials by image analysis. *Polymers Composites* **11,** 274–279.

Zhu, M. and Achenbach, J. D. (1991) Radial matrix cracking and interphase failure in transversely loaded fiber composites. *Mechanics Materials* **11,** 347–356.